Economic Geology, v. 111, pp. 1397–1410

Hydrothermal Alteration Revealed by Apatite Luminescence and Chemistry: A Potential Indicator Mineral for Exploring Covered Porphyry Copper Deposits*

Farhad Bouzari,† Craig J.R. Hart, Thomas Bissig, and Shaun Barker

Mineral Deposit Research Unit, Department of Earth, Ocean and Atmospheric Sciences, University of British Columbia, Vancouver, BC, Canada V6T 1Z4

Abstract

Apatite is a common resistate mineral occurring in a range of host rocks and ore-related hydrothermal alteration assemblages. Apatite in several porphyry copper deposits in British Columbia has a unique set of physical and compositional characteristics that can be used to evaluate the chemical conditions of magmas that formed the causative intrusions or associated hydrothermal alteration.

Apatite under visible light and SEM shows no notable variations between unaltered and altered varieties but cathodoluminescence reveals significant differences. Apatite in unaltered rocks displays yellow, yellow-brown, and brown luminescence, whereas in K silicate-altered rocks apatite displays a characteristic green luminescence. The green-luminescent apatite replaces yellow- or brown-luminescent apatite and locally overgrows it. Apatite occurring with muscovite (i.e., phyllic)-altered rocks displays characteristic gray luminescence.

The chemistry of apatite, as determined by electron microprobe and laser ICP-MS analyses, directly reflects its alteration and luminescence. The unaltered yellow-luminescent apatite has high concentrations of Mn (0.3–0.5 wt % MnO) and a high Mn/Fe ratio (>1), whereas the brown-luminescent apatite has low Mn, but higher concentrations of S and REE + Y. The green K silicate alteration-related luminescence is caused by lower Mn/Fe ratios (ca. 1) along with depletions of other trace elements such as Cl, S, and Na. Gray-luminescent apatite occurring with muscovite-altered rocks results from significant Mn loss (<0.15% MnO) contemporaneous with depletion in Na, S, Cl, and REE during low pH phyllic alteration in calc-alkalic porphyry deposits.

The correlation between apatite texture, luminescence, and chemical composition with the type and intensity of porphyry alteration offers a potentially fast and effective method to utilize it as an indicator for porphyry mineralization in a range of exploration materials including soils, regoliths, and heavy mineral concentrates from glacial and fluvial materials.

Introduction

Indicator minerals are those resistate minerals that have diagnostic features and indicate direct derivation from a mineralized rock. Such minerals are useful for mineral exploration because they persist in the surficial environment despite weathering and transport. Their physical and chemical properties allow them to be easily recovered from exploration samples such as heavy mineral concentrates, so that they can be evaluated and analyzed. Indicator minerals have most successfully been applied to diamond exploration (e.g., Griffin and Ryan, 1995; Averill, 2001; McClenaghan and Kjarsgaard, 2007).

The common occurrence of resistate minerals, such as apatite, rutile, and titanite, as alteration products in many porphyry copper deposits (e.g., Williams and Cesbron, 1977; Czamanske et al., 1981) suggests that these minerals could be utilized as porphyry indicator minerals (PIMS). Such applications have only rarely been considered as exploration tools for porphyry copper deposits (e.g., Force et al., 1984; Averill, 2011; Kelley et al., 2011), possibly because of the lack of descriptive studies that document the features and usefulness of these minerals. Characterization of these minerals in known settings in the porphyry copper environment could therefore provide the basis for a new exploration toolkit.

Apatite [$Ca_5(PO_4)_3F,OH,Cl$] is a common accessory mineral that occurs in the volcanic and plutonic host rocks of many ore deposits, in causative hypabyssal intrusions such as those that form porphyry copper deposits, as well as in many ore or hydrothermal alteration types. Because the apatite crystallographic structure can incorporate a wide range of transition metals, REE, and anions into its structure, apatite can record magma chemistry, fluid evolution, and physiochemical conditions at the time of mineral deposit formation such as Cl:F:OH proportions (Holland, 1972; Roegge et al., 1974; Webster et al., 2009; Patiño Douce et al., 2011; Bath et al., 2013), sulfur content or oxidation state (Boudreau, 1995; Peng et al., 1997; Streck and Dilles, 1998, Parat and Holtz, 2004; Bath et al., 2006; Liaghat and Tosdal, 2008; Boyce and Herving, 2009).

This widespread interest in apatite is mainly related to its association with a causative magma (e.g., Piccoli and Candela, 2002; Webster and Piccoli, 2015) or metamorphism (e.g., Pan et al., 1993; Harlov, 2015). Apatite has also been shown to be a useful tool to evaluate hydrothermal fluid evolution (Williams and Cesbron, 1977; Streck and Dilles, 1998; Hernández, 2009; Bouzari et al., 2011a, b). In this paper, we utilize cathodoluminescence and trace element geochemistry to characterize the nature of magmatic apatite in several porphyry copper deposits in British Columbia, but more importantly demonstrate that apatite can fingerprint the existence, nature, and evolution of a mineralizing hydrothermal fluid. We show that apatite can record hydrothermal fluid interactions during mineralization and alteration and that it has distinct physical

† Corresponding author: e-mail, fbouzari@eos.ubc.ca

*A digital supplement containing Appendices for this paper is available at http://economicgeology.org/ and at http://econgeol.geoscienceworld.org/.

Submitted: September 27, 2015
Accepted: April 4, 2016

and chemical properties that can easily distinguish them from those in barren host rocks. Recognition of such evidence can potentially provide a fast and effective method for mineral exploration, particularly in weathered or covered areas.

British Columbia Porphyry Deposits

Apatites were studied from several porphyry copper deposits in British Columbia (BC), including Highland Valley (2.31 billion metric tons (Bt), production and reserve, at 0.37% Cu, and 0.01% Mo; Byrne et al., 2013), Mount Polley (86 million metric tons (Mt) reserve at 0.30% Cu and 0.30 g/t Au, http://www.imperialmetals.com), Huckleberry (42.2 Mt reserve at 0.33% Cu, http://www.imperialmetals.com), as well as the Endako (33.4 Mt reserve at 0.05% Mo, http://www.thompsoncreekmetals.com) porphyry molybdenum deposit (Fig. 1). These porphyry deposits have a range of characteristics and metal associations with both calc-alkalic and alkalic igneous rocks (McMillan et al., 1995). Calc-alkalic varieties typically have K silicate alteration and abundant quartz stockwork-hosted sulfide mineralization overprinted by sericite alteration, whereas alkalic-associated deposits are characterized by intense K silicate-magnetite alteration, locally with Ca silicate and albite, and generally lack quartz veins and overprinting sericite alteration (Sillitoe, 2010; Bissig and Cooke, 2014). These deposits and prospective exploration areas are variably covered by extensive veneers of till and related glacial sediments (Fig. 2) that increase the difficulty in exploration for new deposits.

The Highland Valley Cu-Mo district consists of a cluster of several deposits in southern BC that formed in the central part of the large, zoned Late Triassic calc-alkaline Guichon Creek batholith which intruded Triassic Nicola Group volcanic and sedimentary rocks (Casselman et al., 1995, Byrne et al. 2013). Most of the ore deposits are hosted in the coarse-grained Bethsaida phase quartz-monzonite to granodiorite (Fig. 3a). K silicate alteration is characterized by pervasive and veinlet-controlled K-feldspar alteration and recrystallized biotite (Fig. 3b). The K silicate alteration commonly occurs as pink K-feldspar (Fig. 3b) which facilitates the mapping of the intensity of the potassic alteration. Much of the sulfide mineralization is associated with overprinting quartz and green muscovite alteration (Fig. 3b, c). Further details of alteration and mineralization are well documented by Casselman et al. (1995), Alva Jimenez (2011), and Byrne et al. (2013).

The Mount Polley Cu-Au deposits in central BC are hosted in Triassic-Jurassic diorite-monzonite intrusions and associated breccia bodies. Alteration progresses outward from a core of K-feldspar-biotite-magnetite-diopside/actinolite to an intermediate K-feldspar-magnetite-biotite-chlorite-calcite zone and an outer zone of albite-epidote-pyrite (Fraser et al., 1995; Logan and Mihalynuk, 2005; Pass et al., 2014; Rees et al., 2014). Fracture-controlled to pervasive "reddening" due to nanoscale hematite inclusions in secondary K-feldspar is common (Rees et al., 2014). The intensity of K silicate alteration can be estimated by abundance of pink and red K-feldspar occurring with secondary biotite and magnetite. Copper

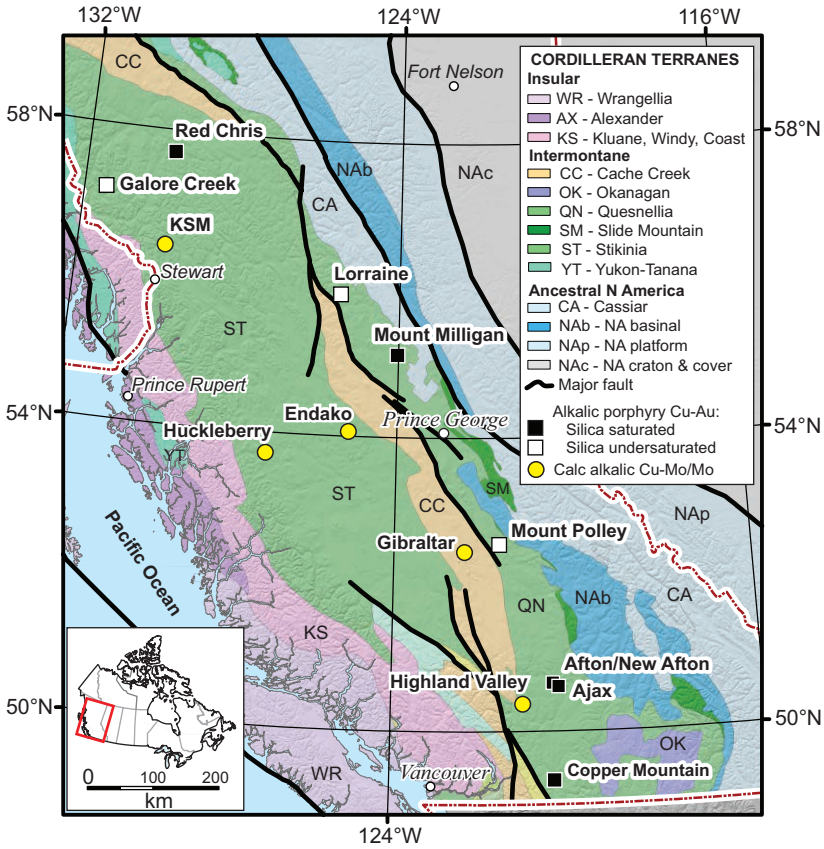

Fig. 1. Location map showing Cordilleran terranes and major porphyry deposits in British Columbia (modified after Bissig and Cooke, 2014).

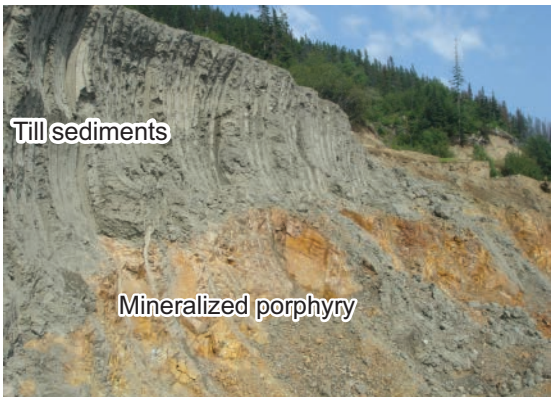

Fig. 2. Bench wall at the margin of the Huckleberry porphyry Cu-Mo deposit, showing thin glacial sediments covering the altered and mineralized bedrock.

and gold values are closely correlated with high magnetite concentrations (Deyell and Tosdal, 2005).

The Huckleberry Cu-Mo porphyry deposit is hosted in Jurassic andesite and dacite volcanic rocks and tuffs, which are intruded by at least two small stocks of Late Cretaceous porphyritic hornblende-biotite-feldspar granodiorite. Mineralization is closely associated with intense fine-grained biotite-albite alteration (also commonly referred to as hornfels by mine geologists) with minor K-feldspar, amphibole, and chlorite (Jackson and Illerbrun, 1995).

The Endako Mo deposit is hosted within the composite calc-alkaline Endako batholith that ranges in composition from diorite, to gabbro, granodiorite, and monzogranite (Whalen et al., 2001). The mineralization occurs within the central quartz-monzonite and is associated with early stage K-feldspar and biotite alteration and subsequent quartz-sericite-pyrite assemblage (Bysouth and Wong, 1995; Selby et al., 2000; Villeneuve et al., 2001).

Apatite

The apatite group minerals belong to the apatite supergroup (Pasero et al., 2010) with a chemical formula of $M1_2M2_3(TO_4)_3X$ and include hexagonal and pseudohexagonal phosphates, arsenates, and vanadates containing the same dominant element in the M1 and M2 sites, and having P, V, or As in the T site. Most common among apatite group minerals are fluorapatite, chlorapatite, and hydroxylapatite. In this paper, the name "apatite" will refer to the three calcium phosphate apatites, and solid solutions among them, with the general formula $Ca_5(PO_4)_3(F,Cl,OH)$. Apatite structure can incorporate a wide range of transition metals, REE, and anions into its structure. Some common substitutions occurring in apatite are as follows (Elliot, 1994; Waychunas, 2002; Hughes and Rakovan, 2015): Sr^{2+}, Mn^{2+}, Fe^{2+}, REE, Y^{3+}, $Na^+ \Leftrightarrow Ca^{2+}$; $Si4^+$, As^{5+}, S^{6+} and $C^{4+} \Leftrightarrow P^{5+}$; Cl^- and $OH^- \Leftrightarrow F^-$; $2Ca^{2+} \Leftrightarrow Na^+ + REE^{3+}$; and $Ca^{2+} + P^{5+} \Leftrightarrow REE^{3+} + Si^{4+}$.

Apatite in ore systems

Apatite can be used to identify features and process that are important in ore systems. Trace element compositions of apatite have been used to recognize the characteristics of mantle fluids, assimilation and degree of fractionation, as well as the oxidation state of magma (Tepper and Kuehner, 1999; Belousova et al., 2002; O'Reilly and Griffin, 2000; Patiño Douce et al., 2011;). Studies on apatite from the Yerington batholith, Nevada (Streck and Dilles, 1998), Galore Creek (Liaghat and Tosdal, 2008), and Mount Polley porphyry Cu-Au, deposits British Columbia (Bath et al., 2006), demonstrated that zoned magmatic apatites may have sulfur-rich cores that abruptly change to sulfur-poor rims, indicating that early sulfate-rich magma evolved to sulfate-poor magma via crystallization of anhydrite.

Bath et al. (2006) demonstrated that apatite crystals from Mount Polley show fractured inclusion-rich cores and fracture-free inclusion-poor rims with cores enriched in sulfur (4,000–5,500 ppm) compared to crystal rims (2,000–3,500 ppm). The

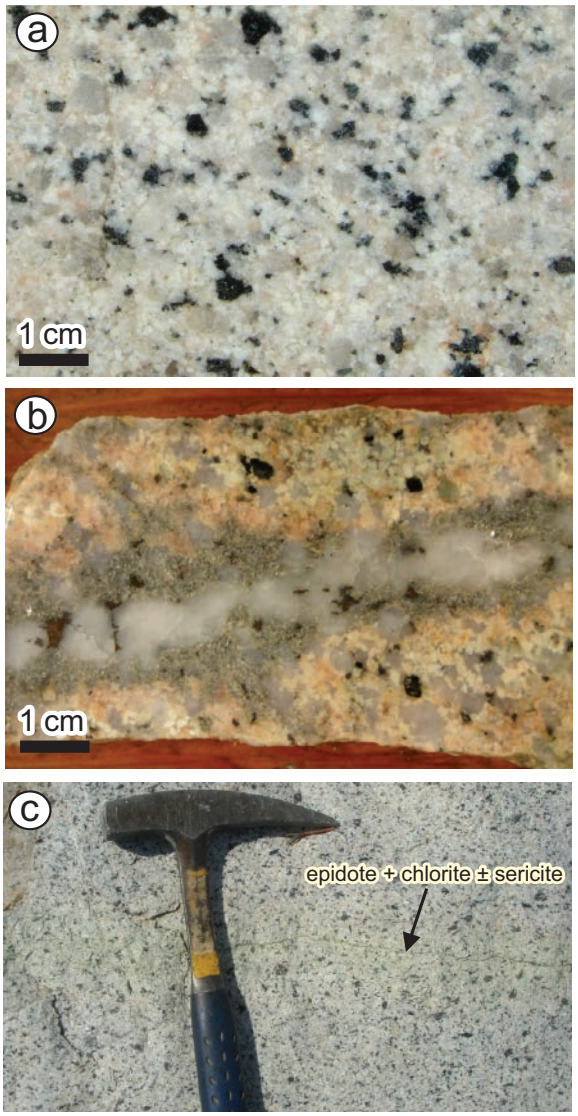

Fig. 3. Samples of the unaltered and altered host rocks at Highland Valley. (a). Unaltered Bethsaida phase with compositions ranging from quartz-monzonite to granodiorite, characteristic rounded quartz phenocrysts, and abundant coarse biotite and plagioclase phenocrysts (ALW-5). (b). Altered Bethsaida phase showing quartz-chalcopyrite-bornite vein with green muscovite alteration halo overprinting earlier K feldspar (pink) alteration (HLV-3b). (c). Weakly altered granodiorite at the margin of the Bethlehem deposit, Highland Valley, with minor secondary biotite after mafic minerals and cut by a thin epidote-chlorite-(sericite) veinlet (BET-1).

decrease in the solubility of sulfur into apatite was attributed to the fluids/melt becoming more reduced, decrease in pressure, increase in temperature, and/or decrease of sulfur within the melt/fluids (Bath et al., 2006).

Moreover, apatites associated with porphyry copper deposits are commonly Cl rich (e.g., Roegge et al., 1974). Thus, apatite can be used as a record for chloride content of the crystalizing melt which may have played a key role in transporting copper (Holland, 1972). Bath et al. (2013), in a study of the East Repulse gold deposit, Australia, showed that fluorine content of apatite decreases at shallower levels in the mineralized zone and suggested that apatite can be used to show pathways of oxidizing fluids. More recently, Ding et al. (2015) used apatite major and trace element concentrations and $^{87}Sr/^{86}Sr$ ratios in southern China to show that the granodiorite porphyry intrusions related to Cu-Pb-Zn mineralization were oxidized, whereas those related to W and Sn deposits were moderately oxidized to reduced.

Apatite luminescence

Luminescence is a property of apatite that is caused by transition metal, REE, and anion substitutions (Waychunas, 2002). Apatite is readily stimulated to luminescence under ultraviolet (UV) light, i.e., fluorescence, or by an electron beam, i.e., cathodoluminescence (CL). Early work by Williams and Cesbron (1977) showed that apatite from porphyry copper deposits displays a characteristic bright orange fluorescence under UV light and displays a complicated history of corrosion and redeposition. They showed that apatite with such characteristics could commonly be detected up to 1 km away from the intrusive core of a mineralized system. Other studies showed that apatites from different deposit types display diagnostic CL emissions. For example, Mariano (1988) and Kempe and Götze (2002) have shown that apatite from mineralization related to carbonatites commonly displays blue CL, and that from peralkaline syenite has pink-violet CL due to activation by trace quantities of rare earth element ions (Ce^{3+}, Eu^{2+}, Sm^{3+}, Dy^{3+}, and Nd^{3+}), whereas those from P-rich granite show strong Mn^{2+}-activated yellow-greenish luminescence. Therefore, luminescence provides a powerful tool to study internal structures and alteration features in apatite in detail, and obtain rapid and essential information on rock formation and mineralization processes.

Materials and Methods

Sampling

Samples were selected from different, well-characterized alteration assemblages and unaltered host rocks at Highland Valley (33 samples), Mount Polley (8), Huckleberry (7), as well as the Endako (6) porphyry molybdenum deposit to determine and characterize the occurrence of resistate minerals.

Samples were evaluated petrographically employing optical and CL microscopy and scanning electron microscopy (SEM) to characterize the abundance and physical properties of apatite, including shape, size, color, and luminescence. Selected grains were analyzed by electron-probe microanalysis (EPMA) and laser ablation inductively coupled plasma mass spectrometry (LA-ICP-MS) for their major and trace element compositions in order to test whether there are key chemical features in apatite that are unique to mineralized porphyry copper deposits. All analyses were conducted at the Department of Earth, Ocean and Atmospheric Sciences, University of British Columbia, Canada.

Methods

A Cambridge Image Technology Ltd. MK 4A model cold CL stage mounted on a petrographic microscope was used to study the internal textures of the apatite grains. The samples were irradiated in a vacuum chamber with an electron beam of approximately 15 kV and the current set at 350 to 500 μA. Petrographic studies of apatite grains under transmitted light, SEM, and CL showed that most grains did not have obvious inclusions, and those inclusions that could be observed were small in size (<0.5 μm). Areas suspected of having inclusions were avoided during the analyses. Electron-probe microanalyses of apatite were conducted using a fully automated CAMECA SX-50 instrument, operating in the wavelength-dispersion mode with the following operating conditions: excitation voltage, 15 kV; beam current, 10 nA; peak count time, 20 s (40 s for F, Cl); background count-time, 10 s (20 s for Cl); spot diameter of 10 μm for improved detection of more volatile elements or elements thought to be affected by diffusion processes such as F, Cl, and Na (Stormer et al., 1993). For the elements considered, the following standards, X-ray lines, and crystals were used: albite, Na$K\alpha$, TAP; kyanite, Al$K\alpha$, TAP; diopside, Mg$K\alpha$, TAP; apatite, P$K\alpha$, TAP; apatite, Ca$K\alpha$, PET; barite, S$K\alpha$, PET; synthetic rhodonite, Mn$K\alpha$, LIF; $SrTiO_3$, Sr$L\alpha$, TAP, topas, F$K\alpha$, TAP; scapolite, and Cl$K\alpha$, PET. Data reduction involved the "PAP" $\phi(\rho Z)$ method (Pouchou and Pichoir, 1985).

Three standard deviations (99.7% confidence level) were used for the calculation of detection limits that are shown in elecronic Appendix 1. Analyses with values below 99.7% confidence level are assumed to be part of background and are not reported. These values however are displayed graphically to show the relative concentrations in various types of luminescent apatite with those that fall below detection limit. Measurements for F are thought to be inaccurate because of the effects of crystal orientations (Stormer et al., 1993) and therefore the F values are not reported. The low totals (95–99%) were due to not accounting for F and other elements that were not analyzed, such as H (OH). Apatite formulae were calculated on the basis of five atoms of Al, Ce, Fe, Mn, Mg, Ca, Sr, and Na. We assumed that Si and S substitute for P (Elliot, 1994). Stoichiometry and total values were used to determine acceptance of each analyses. Because the Al_2O_3 contents of apatite are typically close to zero (e.g., Peng et al., 1997), the Al concentrations were used to determine any contamination by inclusions or other phases. In total, 162 spots were analyzed and three of them were rejected because of contamination.

LA-ICP-MS analyses were carried out using a Resonetics m50-LR 193 nm excimer laser coupled to an Agilent 7700x ICPMS with laser diameter of approximately 15 μm. An ablation time was 40 s with He gas flow (750 ml/min He and 2ml/min N2). Thirty-two masses were analyzed in this study, including ^{43}Ca as the internal standard using the concentrations obtained by EPMA. Glitter 4.0 software was used to determine elemental concentrations using an NIST SRM 612 glass standard for external standardization. Intervals for data

reduction were chosen based on the flattest part of the ^{43}Ca plateau, typically ~2 s after the laser turned on and around 2 s before the laser was turned off. During the data reduction a careful check on the multielement mass spectra eliminated any possible impurities that may have been encountered across the depth profile of each laser-ablated area by assessing the ^{43}Ca profile and inspecting for depressions, and examining for spikes of other masses that indicated the presence of inclusions. In total, four of the 38 spot analyses were rejected. The precision and accuracy of the analyses undertaken during this study are better than ±15%. Results and detection limits are shown in Appendix 1. If the elemental concentrations of LA-ICP-MS data were below detection limits, for the purpose of graphic display of data, value of half of detection limit was used.

Textural Characteristics

Apatite as a primary igneous mineral commonly displays euhedral crystal shape and its hexagonal form is distinctive. However, small apatite grains surrounded by quartz or feldspar are difficult to recognize under the optical transmitted light (TL) microscope. Apatite commonly appears homogeneous if examined under the optical petrographic microscope or the SEM. However, under cathodoluminescence, apatite shows a wide range of colors and textures depending on its origin and alteration that may have affected it. As a result, most observations and descriptions of apatite textures presented here are based on its luminescence properties.

Apatite in unaltered host rocks

Apatite in unaltered host rocks, i.e., magmatic apatite, occurs as homogeneous euhedral grains 100 to 200 μm in diameter. Smaller grains (<10 μm) locally occur as inclusions in other minerals, such as in magnetite. Under CL, apatites in unaltered granodiorite at Highland Valley commonly display strong luminescence of yellow to yellow-green (Fig. 4a).

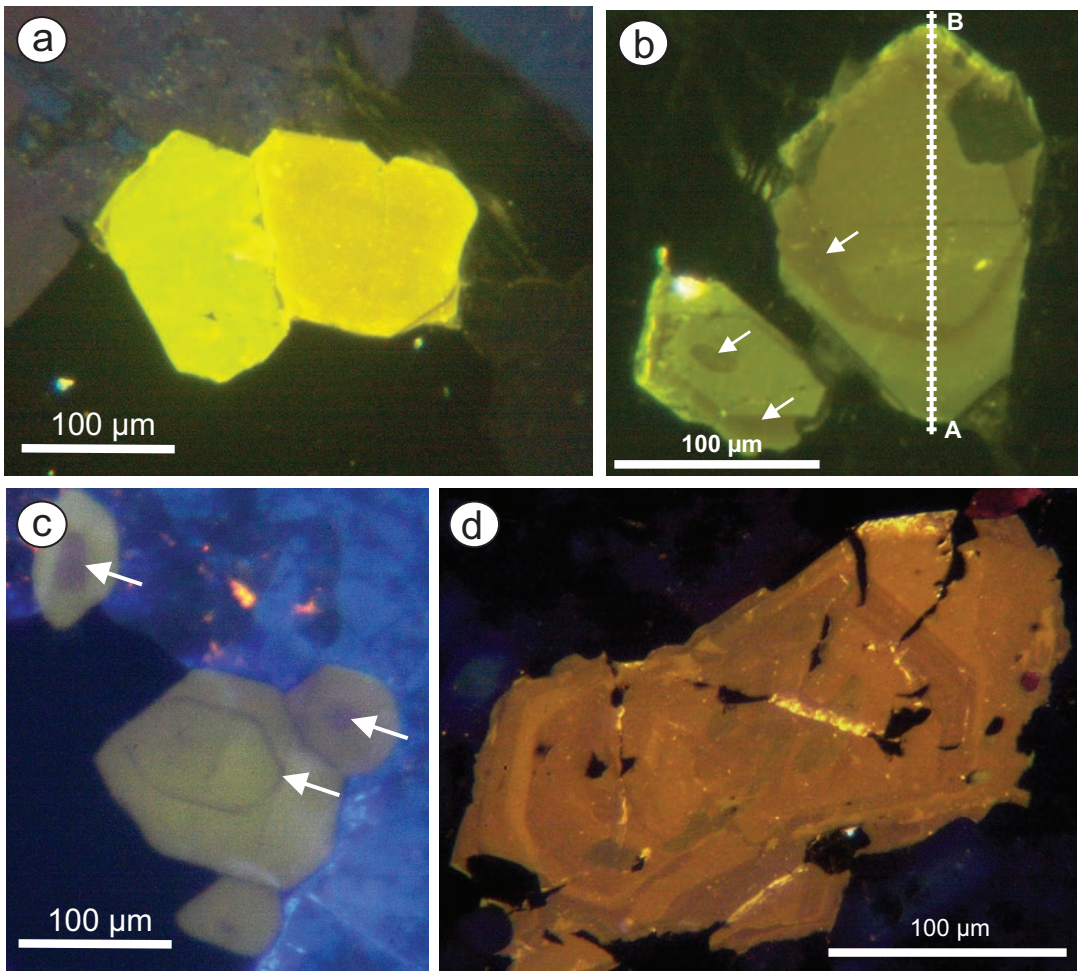

Fig. 4. Cathodoluminescence images of apatites from unaltered host rocks. (a) Two grains of apatite with uniform yellow and yellow-pale-green luminescence in unaltered Bethsaida granodiorite, Highland Valley (ALW-5). (b). Apatite grains in unaltered Bethlehem granodiorite with a light-brown core, a distinct dark-brown zone and a more green-brown CL at the rim. The smaller apatite grain, in the lower-left side of the photo, shows a similar relationship but with a dark-brown CL in the core as well. Moreover, it shows that the dark-brown zone formed after euhedral crystallization of the apatite. A-B line indicates the profile along which 42 spots were analyzed (BET-1). (c). Apatite from unaltered porphyritic monzonite of the Bootjack Stock, Mount Polley, showing zoned yellow-brown luminescence with a brownish zone (see arrows) occurring in the core and as a narrow zone between the core and rim (PTB042). (d). Apatite from unaltered granodiorite host rocks, Huckleberry, showing zoned brown to orange luminescence (HDM024).

Although many grains have homogeneous luminescence, some apatite grains show zoning with a yellow to light-brown core and a distinctive dark-brown zone/band or rim (Fig. 4b).

At Mount Polley, unaltered monzonitic host rocks have zoned yellow-brown-luminescent apatite with more brownish phases occurring in the core, or as one or two narrow zones in the middle or at the rim of the apatite crystal (Fig. 4c). Apatite in the least altered granodiorite host rock at Huckleberry displays orange to yellow-brown luminescence, commonly with fine zoning (Fig. 4d). Samples of unaltered quartz monzonite host rocks from the Endako deposit were not available, but examination of the least altered host rocks reveals apatites with remnants of brown-yellow luminescence cores with green rims. Thus, magmatic apatites in these porphyry deposits are homogeneous or concentrically zoned and display yellow to orange and brown luminescence.

Apatite with K silicate alteration

Apatite in K silicate-altered granodiorite at Highland Valley appears similar to that occurring with unaltered granodiorite when examined using a polarizing microscope and SEM (Fig. 5a, c). However, CL microscopy reveals that apatites in K silicate-altered host rocks display green luminescence. The green luminescence preferentially occurs on the outside margins of the crystals and along fractures within weakly altered apatite (Fig. 5b), and more pervasively as replacements of the entire grain in strongly altered samples (Fig. 6b).

Apatite in K silicate-magnetite-altered rocks at Mount Polley shows bright green luminescence where it has replaced or overgrown brown-luminescent apatite (Fig. 6a). The occurrence, abundance, and intensity of green-luminescent apatite correlate with the intensity of the K silicate alteration. The green-luminescent apatite at Mount Polley is similar to that observed in K silicate-altered rock at Highland Valley.

Apatite occurring with biotite-albite-altered rocks at Huckleberry has orange to red-brown luminescence that has been partially replaced by green and green-brown-luminescent apatite. However, unlike simple replacement or overgrowth of green-luminescent apatite, the K silicate-altered apatite at Huckleberry displays a complex texture of coalescing patches of green luminescent with remnants of red-brown-luminescent apatite (Fig. 6c). Endako apatites occurring with K-feldspar-altered rocks display dominantly green luminescence with remnants of brown-yellow-luminescent apatite commonly preserved (Fig. 6d).

Apatite with muscovite (phyllic) alteration

Apatite in green muscovite-altered and mineralized rocks at Highland Valley (Fig. 3b) displays a distinct dull gray luminescence. The gray-luminescent apatite overprinted and replaced the green-luminescent apatites (Fig. 6b) that are remnants of the K silicate alteration. Figure 6b also shows a narrow rim of green-brown apatite that has mantled both green and gray apatites. This suggests that K silicate-related apatite locally formed after muscovite-related apatite. Apatite occurring in intense pervasive muscovite-altered rocks has been replaced by gray-luminescent apatite producing a "messy" texture (Fig. 6e) with zones and bodies of green-gray to dark gray-luminescent apatite. Luminescence zoning on both sides of a microfracture-hosting chalcopyrite and cutting through apatite grains (Fig. 6f) is evidence of a fluid that altered the apatite during muscovite alteration and deposited sulfides. The overprinting phyllic alteration at the Endako Mo deposit was not studied, and phyllic alteration at the Huckleberry Cu-Mo deposit is only weakly developed. Similarly, gray-luminescent apatite is largely absent in the Mount Polley alkalic deposit, where widespread phyllic alteration is lacking.

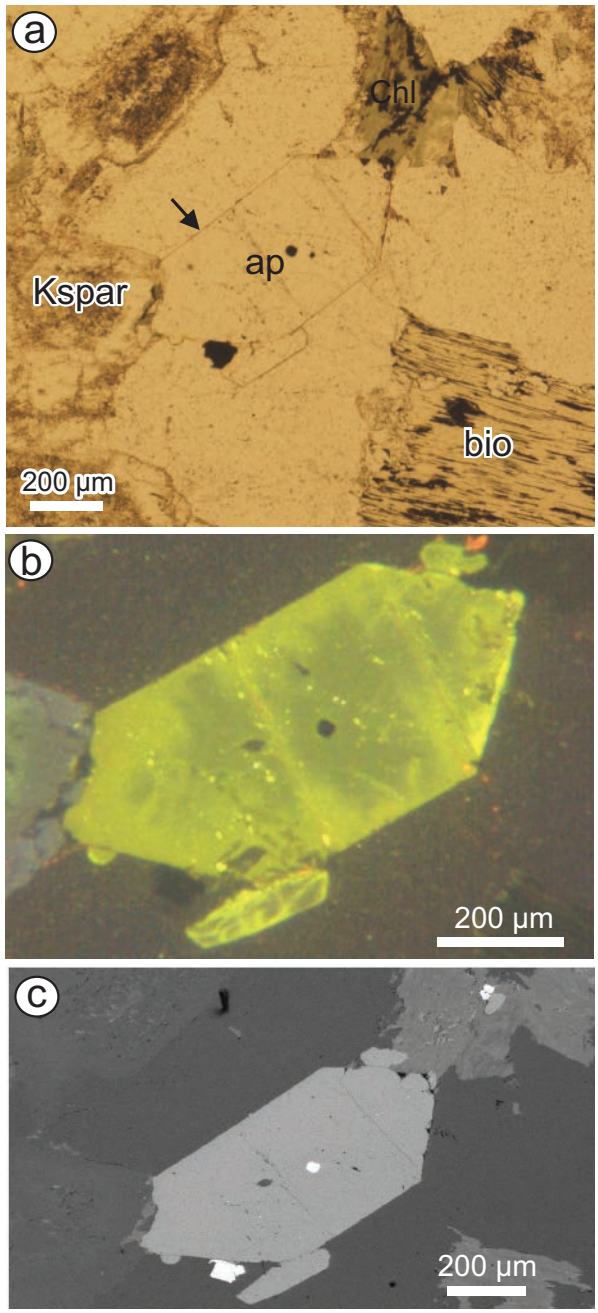

Fig. 5. Highland Valley apatite associated with K silicate alteration. (a). Plane-polarized photomicrograph showing apatite crystal surrounded by quartz and K feldspar and weakly altered biotite and minor sulfide. (b). Cathodoluminescence image of the same apatite grain showing that the dull yellow-brown apatite is replaced by a brighter green-luminescent apatite at the rims and along fractures. (c). SEM image of the same apatite grain showing no internal structure. Abbreviations: ap = apatite, bio = biotite, chl = chlorite, Kspar = K feldspar.

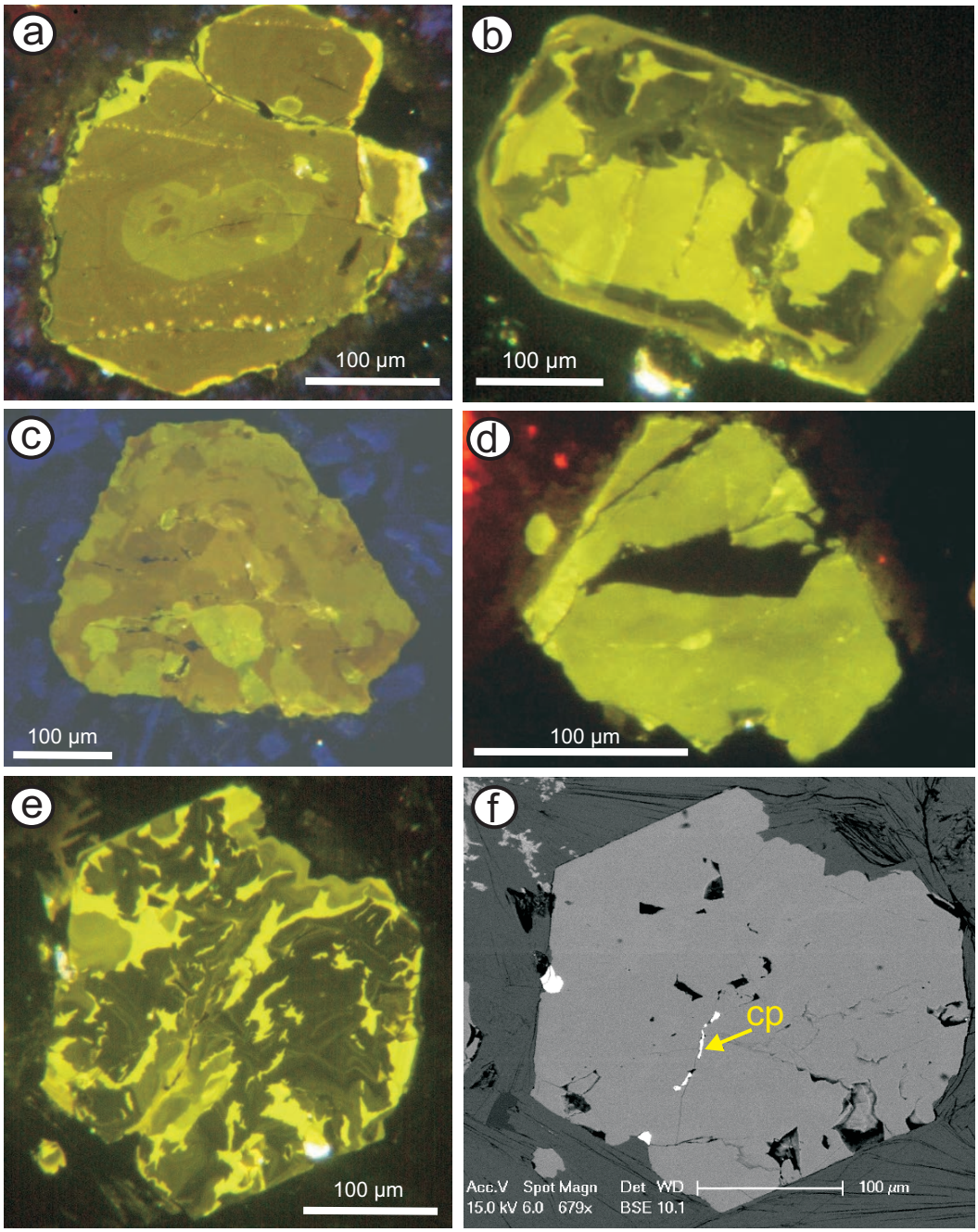

Fig. 6. Cathodoluminescence images of apatites from altered host rocks. (a) Mount Polley apatite occurring with K feldspar + magnetite alteration, showing that green-luminescent apatite has overgrown and locally replaced brown-luminescent apatite (PTB045). (b). Apatite grain occurring with K silicate alteration overprinted by phyllic alteration, showing an early bright green-luminescent apatite cut by dull gray-luminescent apatite. Note that thin green-brown apatite has formed at the rim, presumably after the gray apatite. (c). Huckleberry apatite occurring with K feldspar alteration and sulfide mineralization, showing that brown-luminescent apatite has been replaced by complex bodies of green-luminescent apatite (HDM022-2). (d). Endako apatite occurring with typical K-feldspar alteration, showing dominantly green luminescence with remnant of brown-green-luminescent apatite (EDM 026). (e). Apatite occurring with strong pervasive coarse muscovite and chalcopyrite alteration at Highland Valley, showing that bright green-luminescent apatite is replaced by a variety of dull gray-luminescent apatite phases with fine zoning patterns (ALW-8). (f). SEM image of the above apatite grain showing no internal texture—the very bright phase at the rim and inside the apatite is chalcopyrite (cp), which has formed within a microfracture that has an envelope of green- to gray-luminescent apatite. Acc.V = accelerating voltage (15 Kv), BSE = backscattered electron, Det = detector, Magn = magnification (679×), Spot = refers to specimen current (8–10 nanoamperes), WD = working distance (10.1 mm)

Phyllic alteration at Mount Polley is volumetrically insignificant, being restricted mostly to narrow halos (~1 m wide) around faults.

Chemical Characteristics

Apatite can contain high concentrations of REE, Sr, Mn, Na, U, and Th, and other trace elements in its structure, making it potentially a sensitive recorder of the trace element chemistry of the rock system (Fleet and Pan, 1997). The incorporation of trace elements in accessory apatite depends on the geologic environment of host rock formation such as the SiO_2 activity, f_{O_2}, total alkalis, the aluminum saturation index (ASI) and subsequent alteration processes (e.g., Sha and Chappell, 1999; Belousova et al., 2002). These parameters, particularly the relationship between fractionation and oxidation state, are critical to the development of magma-related porphyry and hydrothermal ore systems (Blevin and Chappell, 1995; Webster and Piccoli, 2015). Thus, the geochemical signatures recognized in apatite from specific rock types and alteration assemblages can potentially provide discriminators that make apatite useful as an indicator mineral in mineral exploration.

To better understand the chemical changes, patterns, and relationships observed in the CL, and to provide additional discriminating criteria in apatite related to porphyry mineralization, selected grains were analyzed for major and trace elements and results were compared with alteration types, textural characteristics, and luminescence color (e.g., yellow, brown, green or gray). Appendixes 1 and 2 show results of apatite analyses with concentrations in weight percent (wt %) and per formula unit (pfu) for EPMA and ppm for LA-ICP-MS analyses.

Electron probe microanalyses data indicate that analyzed grains belong to the apatite group and because of lack of significant amount of Ba, As, Sr, Pb, and V (Pasero et al., 2010), all of grains are calcium phosphate with F, probably OH and minor Cl. Results show that the Cl content is low (0.1–0.2%) but because of difficulty in measuring F content in apatite (see above), it is not possible to differentiate between fluorapatite and hydroxylapatite. As a result, all the mineral grains analyzed in this study can be best referred to as "apatite" with a formula of $Ca_5(PO_4)$(F, OH, Cl). The compositions of apatites from this study are similar to those that commonly occur in volcanic-plutonic rocks, with compositions between fluorapatite and hydroxylapatite end members (Webster and Piccoli, 2015).

Magmatic apatite composition

Results from the magmatic apatite grains analyses occurring in unaltered host rocks show variations in compositions that correlate with their luminescence. Apatites with yellow luminescence from Highland Valley have high Mn (>0.2% MnO) concentrations and chemically are similar to the apatites occurring in felsic (>70% SiO_2) I-type granite at the Lachlan fold belt, Australia (Sha and Chappell, 1999; Fig. 7). Magmatic apatite grains with brown or orange luminescence from the Mount Polley, Huckleberry, and Endako deposits have lower Mn concentrations, mostly below detection limit (0.15% MnO) and plot near the boundary between felsic and mafic (57–70% SiO_2) I-type granite apatites (Fig. 7). Moreover, magmatic apatite samples with brown luminescence

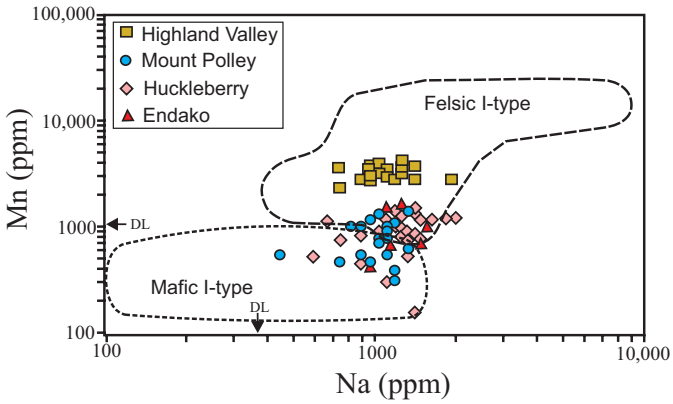

Fig. 7. Binary diagram comparing the Mn-Na composition of apatite in the deposits studied with those occurring with felsic and mafic I-type granitoids from the Lachlan fold belt, Australia (Sha and Chappell, 1999). Yellow-luminescent apatite occurs in the felsic I-type field, whereas brown-luminescent apatites occur near, or probably within, the mafic I-type field. DL = detection limit.

from Mount Polley and Endako commonly have higher sulfur concentrations (0.1–0.4% SO_3) compared to yellow to yellow-brown-luminescent apatite from Highland Valley and Huckleberry (<0.1%). Yellow-luminescent apatites at Highland Valley locally show core, rim, or zones with brown luminescence (Fig. 4b). Analysis of several spots across one apatite grain (Fig. 4b) shows that the yellow-brown CL core is moderately enriched in REE + Y (ca. 4,500 ppm) whereas the dark-brown CL zone is highly enriched in REE + Y (5,000–9,000 ppm; Fig. 8). The rim has light-brown to weak green CL and is largely depleted in REE + Y (Figs. 4b, 8). This is probably related to weak K silicate alteration, characterized by minor secondary biotite after hornblende, or propylitic alteration, characterized by thin epidote-chlorite-minor sericite veinlets at the margin of the deposit (Fig. 3d).

Hydrothermal apatite compositions

Change in Mn/Fe: Manganese is above the detection limit in most apatite samples from Highland Valley. Mn has the greatest concentrations in magmatic yellow-luminescent apatite (0.3–0.5% MnO or 0.025–0.038 pfu Mn) with the K

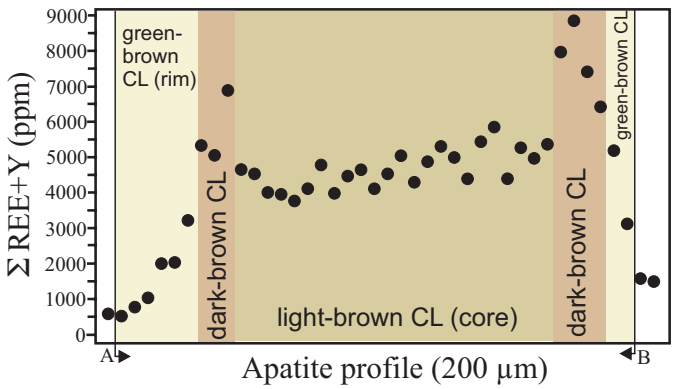

Fig. 8. Variation in trace element composition across a zoned apatite grain (Fig. 4b), showing that the dark-brown CL zone has higher REE concentration. CL = cathodoluminescence.

silicate-altered green-luminescent apatite typically containing less than 0.3% MnO or 0.020 pfu Mn (Fig. 9a). The gray-luminescent apatite occurring with muscovite-altered rocks has characteristically the lowest Mn concentrations near or below the detection limit of 0.15% MnO or 0.010 pfu Mn (Fig. 9a). The decrease in Mn concentration correlates with the decrease in Mn/Fe ratio (see below).

Sodium, sulfur, and chlorine depletion: Comparisons of chemical compositions of magmatic and hydrothermal apatite at Highland Valley show that nearly all magmatic apatites have Na contents of 0.1 to 0.2% Na_2O (0.020–0.040 pfu Na), whereas green-luminescent K silicate-altered apatites contain less than 0.020 pfu Na (Fig. 9b). The Na contents of the gray-luminescent apatite are commonly the lowest, generally below the detection limit (0.05% Na_2O or 0.01 pfu). Similar relationships were observed for chlorine (Fig. 9c). Most of the Highland Valley apatite analyses for sulfur were below the detection limit (0.17% SO_3); samples with concentrations above the detection limit were mainly from unaltered rocks with yellow-luminescent apatite. Therefore, hydrothermal apatites consistently have lower concentrations of Na, Cl, and S relative to magmatic apatites, indicating that these elements were depleted from apatite during K silicate and subsequent phyllic hydrothermal alterations. Similar relationships were observed for apatite from Mount Polley, Huckleberry, and Endako (Fig. 10). Thus, comparing magmatic and hydrothermal apatite, the K silicate-altered green-luminescent apatite has lower concentrations of Na and S (commonly below detection limit) than the magmatic brown-luminescent apatite (Fig. 10a-d).

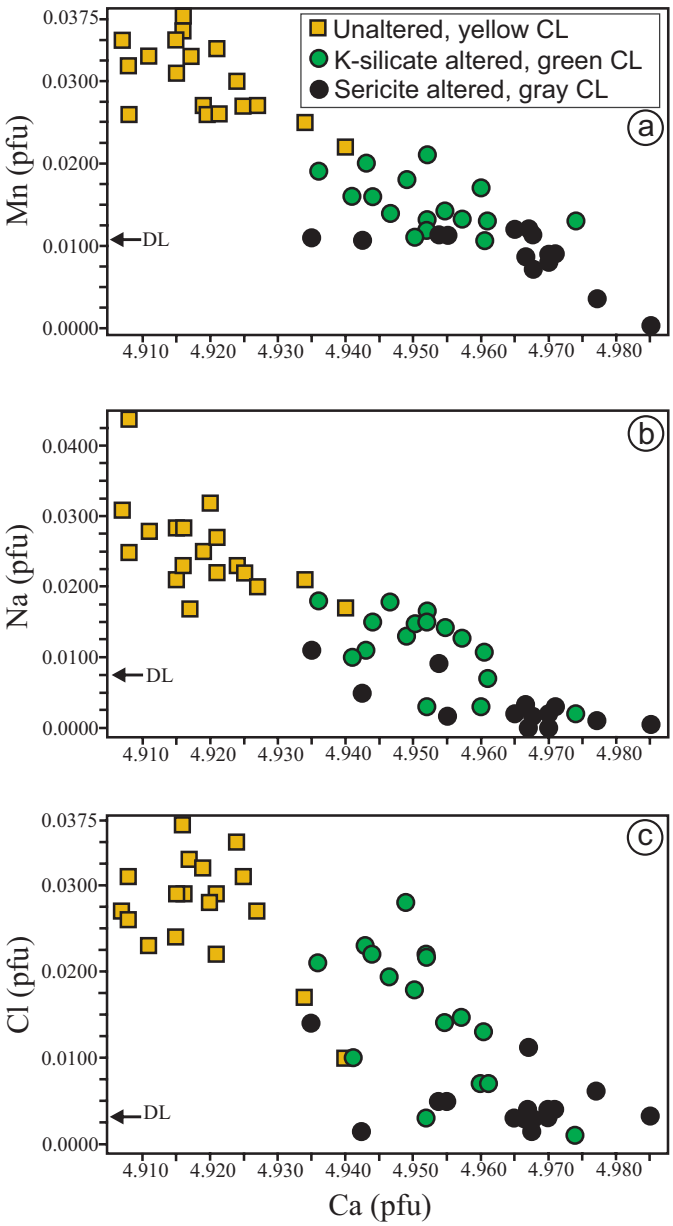

Fig. 9. Trace element composition of apatite with yellow, green and gray luminescence in unaltered and altered host rocks, Highland Valley, showing that altered samples are depleted in Mn, Na, and Cl. CL = cathodoluminescence, DL = detection limit, pfu = per formula unit

REE depletion: Laser ICP-MS analyses of apatite in various alteration assemblages at Highland Valley show that Y and most REE, including Ce, Nd, Sm, Eu, Er, and Yb, have lower concentrations in altered samples (Fig. 11). This depletion occurs in both K silicate- and muscovite-altered assemblages but the latter shows the strongest depletion. Both LREE and HREE are depleted, generating flat REE patterns in the chondrite-normalized spider diagrams for the muscovite-altered samples (Fig. 12). Lanthanum, however, shows weaker depletion and even slight enrichment in K silicate-altered rocks. The magnitude of the Eu anomaly becomes weaker as a result of alteration and depletion of REE, and some samples show a negative Nd anomaly in muscovite-altered rocks (Fig. 12).

Relationships Between Alteration, Apatite Texture, and Chemistry

Our study of apatite from 54 samples representing a range of alteration types and intensities from four porphyry deposits in British Columbia has highlighted several distinct features. Apatite from the unmineralized felsic igneous host rocks typically display yellow and brown luminescence. The strong yellow luminescence is attributed to the higher concentration of Mn relative to Fe (Mn/Fe >1). The Mn-enriched apatites are characteristic of felsic (>70% SiO_2) granites (Sha and Chappell, 1999) such as in the Bethsaida granodiorite phase at Highland Valley (Olade, 1977). Higher Mn and lower S contents in apatites from felsic I- and S-type granites are attributed to the lower oxygen fugacity and higher peraluminosity of these magmas compared to their mafic I-type counterparts (Sha and Chappell, 1999). The yellow-brown to orange-brown-luminescent apatite occurs with largely mafic I-type intrusions that host alkalic porphyry deposits, e.g., Mount Polley diorite and monzonite (49–56% SiO_2, Bath and Logan, 2006), or less felsic calc-alkalic host rocks such as Endako quartz monzonite (ca. 67% SiO_2, Whalen et al., 2001). The brown to orange luminescence in these samples is attributed to their high REE + Y and probably S. Dark-brown cores or zones in apatite (Figs. 4b, 8) are highly enriched in REE. Similar zonation was described in the Karkonosze granitoid pluton, Poland (Lisowiec et al., 2013) and the Idaho batholith, United Stars (Tepper and Kuehner, 1999) where it was attributed to magma-mixing processes.

Apatite occurring with K silicate-altered host rocks in all

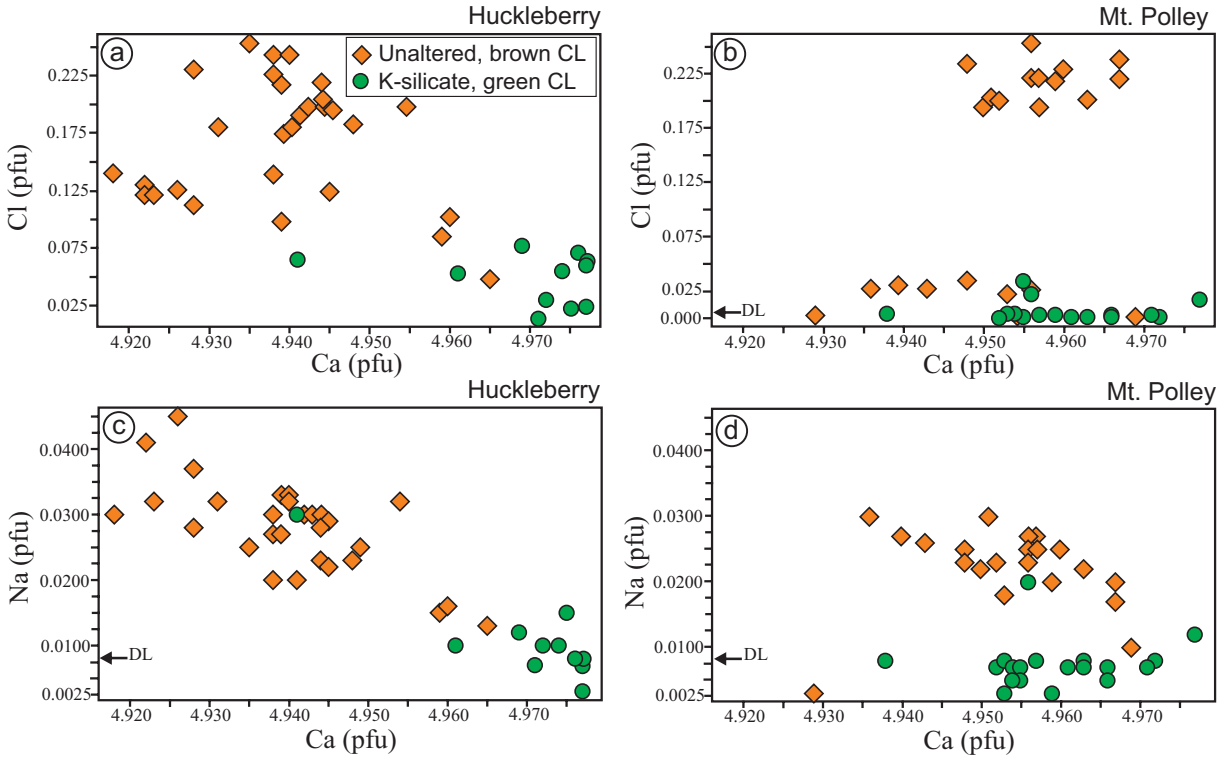

Fig. 10. Trace element composition of brown- and green-luminescent apatite at the Mount Polley and Huckleberry porphyry deposits, showing that altered samples are depleted in Na and Cl. CL = cathodoluminescence, DL = detection limit, pfu = per formula unit

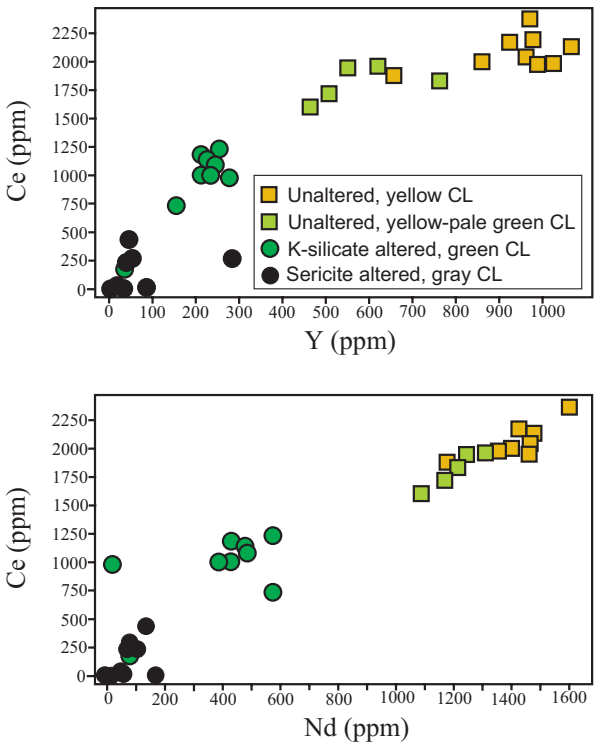

Fig. 11. Ce, Y, and Nd concentration in various types of apatite occurring with unaltered and altered host rocks at Highland Valley. Note that unaltered yellow CL apatite with weak green luminescence has slightly lower REE concentration. Other REE show similar trends. CL = cathodoluminescence.

studied samples from both calc-alkalic and alkalic deposits displays green luminescence. The green-luminescent apatite replaced yellow- or brown- to orange-luminescent apatite, and less commonly occurs as thin overgrowths on magmatic apatite. The green-luminescent apatite formed by progressive depletion of Mn from the apatite Ca site structure, probably contemporaneous with some addition of Fe, causing a decrease in overall Mn/Fe ratio (ca. 1) during K silicate alteration. Kempe and Götze (2002) showed that there is no direct correlation between CL intensity in apatite and absolute concentrations of Mn or Fe. Thus, the control on change in luminescence is the Mn/Fe ratio and not the absolute concentration of Mn or Fe.

Other trace elements such as Na, Cl, and S and REE were depleted during K silicate alteration. More importantly, REE concentrations appear to be sensitive to the degree of hydrothermal alteration compared to other trace elements. Samples in least altered host rocks contain yellow-green-luminescent apatite, either as whole grains or at the rims of yellow-luminescent apatite (Fig. 4b), reflecting very weak K silicate and/or propylitic alterations (see above). These yellow-green-luminescent apatites have lower concentrations of REE compared to other trace elements, which do not show notable changes in concentrations (Figs. 11, 13), suggesting that REE concentration potentially can be used to map distal weak alteration where commonly visible alteration phases are absent and other chemical variations are not easily detectable.

Apatite occurring with muscovite or phyllic alteration displays gray luminescence. The gray-luminescent apatites

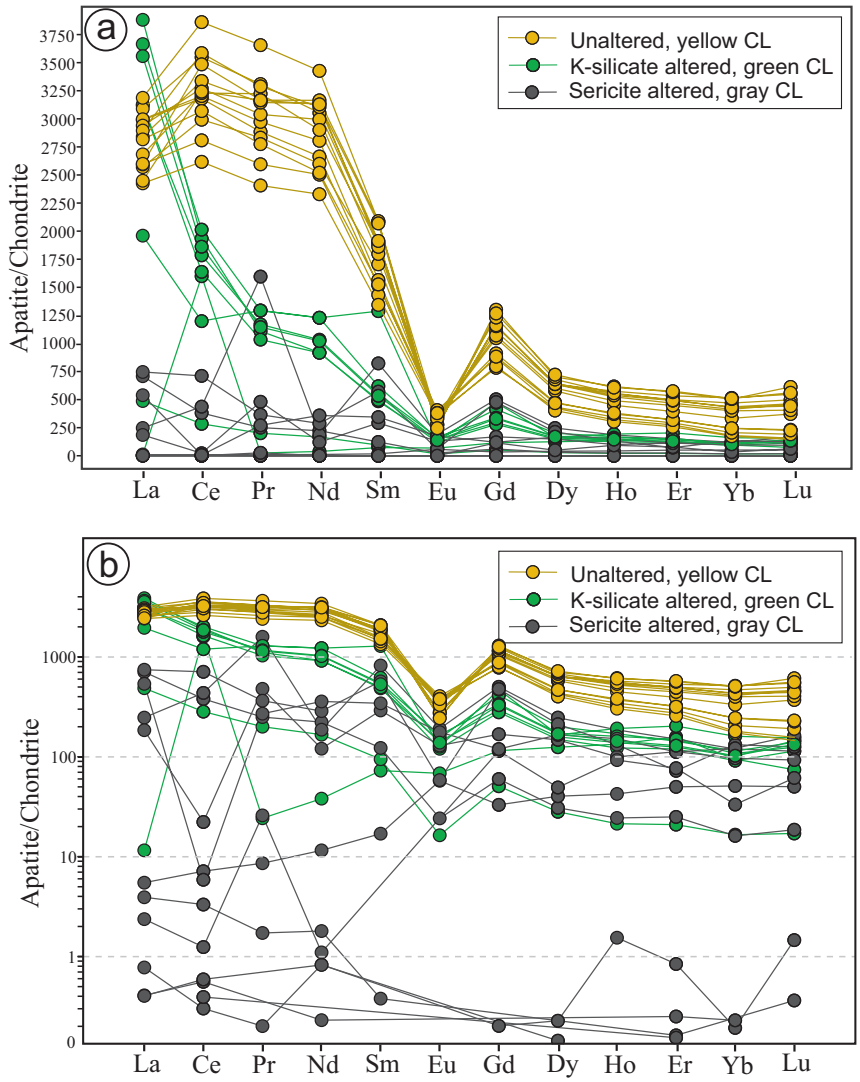

Fig. 12. Chondrite-normalized REE distribution patterns of apatites from Highland Valley granodiorite in normal scale (a) and log scale (b), showing that altered samples are characterized by strong REE depletion and weaker Eu anomaly. Samples with strong phyllic alteration display a flat REE with erratic LREE pattern. Chondrite REE abundances are from Sun and McDonough (1989).

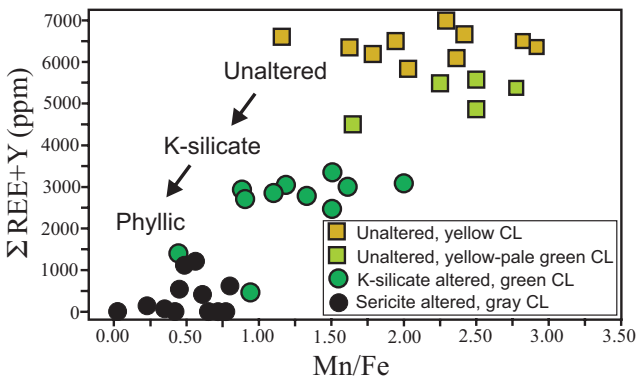

Fig. 13. Correlation of the apatite luminescence and alteration with the Mn/Fe ratio and abundance of REE. Very weak K silicate alteration of apatite occurs as slightly green-, yellow-, luminescent apatite. The pale green-yellow luminescent apatites have slightly but distinctly lower REE. K silicate-altered samples, have green luminescence, and a lower REE and Mn/Fe ratio. Sericite-altered apatites have gray luminescence and lowest REE and Mn/Fe.

replace green-luminescent apatite. At Highland Valley, a small fracture in apatite, filled with sulfide minerals, and with a halo of gray-luminescent apatite overprinting green-luminescent apatite shows that hydrothermal fluids caused the alteration in apatite and deposited sulfide minerals (Fig. 6e, f). The acidic fluids, typical of phyllic alteration in porphyry deposits, significantly depleted Mn, Na, Cl, and REE which in turn resulted in the loss of luminescence, thus producing the gray-luminescent apatite.

Although our database only represents porphyries from a limited geographic and temporal range, it suggests that apatite luminescence and chemical compositions can provide a new approach for fingerprinting porphyry-related hydrothermal alteration. K silicate alteration in both calc-alkalic and alkalic porphyry deposits is characterized by green-luminescent apatite. The green-luminescent apatite has lower Mn/Fe ratio, REE (Fig. 13), Na, and S (Fig. 14) relative to magmatic apatite. Phyllic alteration in the calc-alkalic deposits generated

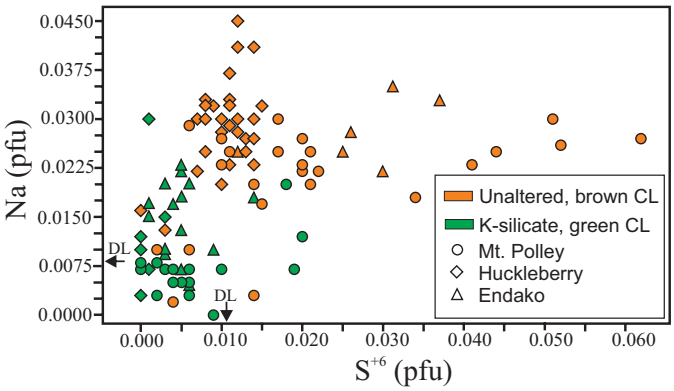

Fig. 14. Binary diagram showing correlation of the apatite luminescence and alteration with the concentration of Na_2O and SO_3. K silicate-altered samples have lower Na and S. CL = cathodoluminescence, DL = detection limit, pfu = per formula unit.

gray-luminescent apatite characterized by depleted trace elements, particularly Mn and REE (Fig. 13). These results now need to be tested in other porphyry provinces and other protoliths, in order to demonstrate the robustness of the technique.

Exploration Implications

Apatite is a recorder of hydrothermal processes in porphyry copper deposits. The correlation between hydrothermal mineral assemblages and apatite luminescence and chemistry, particularly Mn/Fe, Na, S, and REE concentrations, suggests that textural and chemical characteristics of apatite can be used to identify specific types and indicate intensity of hydrothermal alteration related to porphyry copper deposits. Recognition of features that are directly related to mineralizing processes, in a range of exploration materials such as soils, regolith, or heavy mineral concentrates from glacial and fluvial materials, provides a promising tool for explorers to link back to a porphyry deposit, related causative intrusion or alteration assemblage. This is particularly useful where common silicate alteration minerals are extensively weathered to clay during surficial processes. Therefore, CL study on apatite grains concentrates can provide a fast screening tool to assess existence of hydrothermal alteration in bedrock and select more promising areas. This can be followed by further detailed sampling backed by microprobe analyses to investigate specific targets and evaluate types of alteration.

Apatite therefore has the potential to be an effective porphyry indicator mineral. The unique physical and chemical characteristics and properties of apatite along with other resistate minerals that typically occur in porphyry copper deposits, such as red rutile (Williams and Cesbron, 1977; Scott, 2005; Rabbia et al., 2009), Ti-rich garnet (Watson, 1969; Russell et al., 1999; Micko, 2010), rose inclusion-rich zircon (Ballard et al., 2002; Averill, 2007), blond titanite (Nakada, 1991; Piccoli, et al., 2000; Celis et al., 2015), and magnetite (Canil et al., 2015; Nadoll et al., 2015), indicate that with further characterization, these minerals can contribute in developing a porphyry indicator minerals methodology akin to accessory minerals and G10 garnets widely used for diamond exploration.

Acknowledgments

We would like to thank Teck (Highland Valley deposit) and Imperial Metals (Mount Polley and Huckleberry deposits) for allowing access and sampling at their properties. Dianne Mitchinson provided samples from Endako. Mati Raudsepp and Edith Czech helped with EPMA and Marghaleray Amini helped with LA-ICP-MS analyses. Geoscience BC is thanked for its generous financial contribution in support of this MDRU contribution no. 367. We also thank David Cooke, Jeffrey Mauk, and an anonymous reviewer as well as the Editor, Larry Meinert, for constructive comments on earlier versions of this manuscript.

REFERENCES

Alva Jimenez, T.R, 2011, Variation in hydrothermal muscovite and chlorite composition in the Highland Valley porphyry Cu-Mo district, British Columbia, Canada: M.Sc. thesis, Vancouver, University of British Columbia, 234 p.

Averill, S.A., 2001, The application of heavy indicator mineralogy in mineral exploration, with emphasis on base metal indicators in glaciated metamorphic and plutonic terrain: Geological Society of London Special Publication 185, p. 69–82.

——2007, Recent advances in base metal indicator mineralogy: An update from Overburden Drilling Management Limited: Explore, v. 134, p. 2–6.

——2011, Viable indicator minerals in surficial sediments for two major base metal deposit types: Ni-Cu-PGE and porphyry Cu: Geochemistry, Exploration, Environment, Analysis, v. 11, p. 279–291.

Ballard, J.R., Palin, J.M., and Campbell, I.H., 2002, Relative oxidation states of magmas inferred from Ce(IV)/Ce(III) in zircon: Application to porphyry copper deposits of northern Chile: Contributions to Mineralogy and Petrology, v. 144, p. 347–364.

Bath, A.B., and Logan, J.M., 2006, Geochemistry of the Late Triassic Bootjack Stock (NTS 093A/12), south-central British Columbia: British Columbia Ministry of Energy, Mines, and Petroleum Geological Fieldwork 2005, Paper 2006-1, 18 p.

Bath, A.B., Logan, J.M. and Kamenetsky, V.S., 2006, Apatite in Cu-sulfide ore from the Mount Polley alkalic porphyry, BC Canada [abs.]: Annual V.M Goldschmidt Conference, 16th, Geochimica et Cosmochimica Acta, v. 70, no. 18, suppl. 1, p. A40.

Bath, A.B., Walshe, J.L., Cloutier, J., Verrall, M., Cleverley, J.S., Pownceby, M.I., Macrae, C.M., Wilson, N.C., Tunjic, J., Nortje, G.S., and Robinson, P., 2013, Biotite and apatite as tools for tracking pathways of oxidized fluids in the Archean East Repulse gold deposit, Australia: Economic Geology, v. 108, p. 667–690.

Belousova, E.A., Griffin, W.L., O'Reilly, S.Y., and Fisher, N.I., 2002, Apatite as an indicator mineral for mineral exploration: trace-element compositions and their relationship to host rock type: Journal of Geochemical Exploration, v. 76, p. 45–69.

Bissig, T., and Cooke, D.R., 2014, Introduction to the special issue devoted to alkalic porphyry Cu-Au and epithermal Au deposits: Economic Geology, v. 109, p. 819–825.

Blevin, P.L., and Chappell, B.W., 1995, Chemistry, origin, and evolution of mineralized granites in the Lachlan fold belt, Australia: The metallogeny of I- and S-type granites: Economic Geology, v. 90, 1604–1619.

Boudreau, A., 1995, Fluid evolution in layered intrusions: Evidence from the chemistry of the halogen-bearing minerals: Geological Society of Canada Short Course 23, p. 25–46.

Bouzari, F., Hart, C.J.R., Barker, S., and Bissig, T., 2011a, Exploration for concealed deposits using porphyry indicator minerals (PIMs): Application of apatite texture and chemistry [abs.]: International Applied Geochemistry Symposium, 25th, Rovaniemi, Finland, Abstracts, p. 89–90.

——2011b, Porphyry indicator minerals (PIMs): Exploration for concealed deposits in central British Columbia: Geoscience BC Report 2011-17, 31 p., URL <http://www.geosciencebc.com/i/project_data/GBC_Report2011–7/GBC_Report2011–07_BCMEM%20OF2011-1.pdf>[November 23, 2012]

Boyce, J.W., and Hervig, R.L., 2009, Apatite as a monitor of late-stage magmatic processes at Volcán Irazú, Costa Rica: Contributions to Mineralogy and Petrology, v. 157, p. 135–145.

Byrne, K., Stock, E., Ryan, J., Johnson, C., Nisenson, J., Alva Jimenez, T., Lapointe, M., Stewart, H., Grubisa, G., and Sykora, S., 2013, Porphyry

Cu-(Mo) deposits in the Highland Valley district, south central British Columbia: Society of Economic Geologists, Field Trip Guidebook Series 44, p. 99–116.
Bysouth, G.D., and Wong, G.Y., 1995, The Endako molybdenum mine, central British Columbia: An update: Canadian Institute of Mining and Metallurgy Special Volume 46, p. 697–703.
Canil, D., Grondahl, C., Lacourse, T., and Pisiak, L. K., 2015, Trace elements in magnetite from porphyry Cu-Mo-Au deposits in British Columbia, Canada: Ore Geology Reviews, v. 72, p. 1116–1128.
Casselman, M.J., McMillan, W.J., and Newman, K.M., 1995, Highland Valley porphyry copper deposits near Kamloops, British Columbia: A review and update with emphasis on the Valley deposit: Canadian Institute of Mining and Metallurgy Special Volume 46, p. 161–191.
Celis, M.A., Bouzari, F., Hart, C.J.R., Bissig, T., and Ferbey, T., 2015, Titanite as a porphyry indicator mineral for alkalic Cu-Au porphyry deposits in south-central British Columbia [abs.]: International Applied Geochemistry Symposium, 27th, Tucson, Arizona, April 20–24, 2015, Abstracts.
Czamanske, G.K., Force, E.R., and Moore, W.J., 1981, Some geologic and potential resource aspects of rutile in porphyry copper deposits: Economic Geology, v. 76, p. 2240–2256.
Deyell, C.L., and Tosdal, R.M., 2005, Alkalic Cu-Au deposits of British Columbia: Sulfur isotope zonation as a guide to mineral exploration: BC Ministry of Energy, Mines and Petroleum Resources Paper 2005-1, p. 191–208.
Ding, T., Ma, D., Lu, J., and Zhang, R, 2015, Apatite in granitoids related to polymetallic mineral deposits in southeastern Hunan Province, Shi-Hang zone, China: Implications for petrogenesis and metallogenesis: Ore Geology Reviews, v. 69, p. 104–117.
Elliot, J.C., 1994, Structure and chemistry of the apatites and other calcium orthophosphates: Elsevier, Amsterdam, 389 p.
Fleet, M.E., and Pan, Y.M., 1997, Rare earth elements in apatite: Uptake from H_2O-bearing phosphate fluoride melts and the role of volatile components: Geochimica et Cosmochimica Acta, v. 61, p. 4745–4760.
Force, E.R., Djaswadi, S., and Van Leeuwen, T., 1984, Exploration for porphyry metal deposits based on rutile distribution: A test in Sumatra: U.S. Geological Survey Bulletin, v. 1558-A.
Fraser, T.M., Stanley, C.R., Nikic, Z.T., Pesalj, R., and Gorc, D., 1995, The Mount Polley copper-gold alkalic porphyry deposit, south-central British Columbia: Canadian Institute of Mining and Metallurgy Special Volume 46, p. 609–622.
Griffin, W.L., and Ryan, C.G., 1995, Trace elements in indicator minerals: Area selection and target evaluation in diamond exploration: Journal of Geochemical Exploration, v. 53, p. 311–337.
Harlov, D.E., 2015, Apatite: A fingerprint for metasomatic processes: Elements, v. 11, p. 171–176.
Hernández, L.B., 2009, Apatita magmatica como monitor de la evolución de volátiles en intrusivos félsicos del área La Huifa-La Negra, Distrito El Teniente: M.Sc. thesis, Santiago de Chile, Universidad de Chile, 227 p.
Holland, H.D., 1972, Granites, solutions, and base metal deposits: Economic Geology, v. 67, p. 281–301.
Hughes, J.M., and Rakovan, J.F., 2015, Structurally robust, chemically diverse: Apatite and apatite supergroup minerals: Elements, v. 11, p. 165–170.
Jackson, A., and Illerbrun, K., 1995, Huckleberry porphyry copper deposit, Tahtsa Lake district, west-central British Columbia: Canadian Institute of Mining and Metallurgy Special Volume 46, p. 313–321
Kelley, K.D., Eppinger, R.G., Lang, J., Smith, S.M., and Fey, D.L., 2011, Porphyry Cu indicator minerals in till as an exploration tool: Example from the giant Pebble porphyry Cu-Au-Mo deposit, Alaska, USA: Geochemistry: Exploration, Environment, Analysis, v. 11, p. 321–334.
Kempe, U., and Götze, J., 2002, Cathodoluminescence (CL) behaviour and crystal chemistry of apatite from rare-metal deposits: Mineralogical Magazine, v. 66, p. 151–172.
Liaghat, S., and Tosdal, R., 2008, Apatite chemical composition and textures as a probe into magmatic conditions at Galore Creek porphyry copper-gold deposit, British Columbia [abs.]: Annual V.M. Goldschmidt Conference, 18th, Geochimica et Cosmochimica Acta, v. 72, no. 12, p. A550.
Lisowiec, K., Słaby, E., and Götze, J., 2013, Cathodoluminescence (CL) of apatite as an insight into magma mixing in the granitoid pluton of Karkonosze, Poland [abs.]: Conference on Raman and Luminescence Spectroscopy in the Earth Sciences, University of Vienna, Austria, Abstracts, p. 67–68.
Logan, J.M., and Mihalynuk, M.G., 2005, Regional geology and setting of the Cariboo, Bell, Springer and Northeast porphyry Cu-Au zones at Mount Polley, south-central British Columbia: BC Ministry of Energy, Mines and Petroleum Resources Paper 2005-1, p. 249–270.
Mariano, A.N., 1988, Some further geological applications of cathodoluminescence, *in* Marshall, D.J., ed., Cathodoluminescence of geological materials: Boston, Unwin Hyman, p. 94–123.
McClenaghan, M.B. and Kjarsgaard, B.A., 2007, Indicator mineral and surficial geochemical exploration methods for kimberlite in glaciated terrain: Examples from Canada: Geological Association of Canada Special Publication 4, p. 983–1006.
McMillan, W.J., Thompson, J.F.H., Hart, C.J.R., and Johnston, S.T., 1995, Regional geological and tectonic setting of porphyry deposits in British Columbia and Yukon Territory: Canadian Institute of Mining and Metallurgy Special Volume 46, p. 40–57.
Micko J., 2010, The geology and genesis of the central zone alkalic copper-gold porphyry deposit, Galore Creek district, northwestern British Columbia, Canada: Ph.D. thesis, Vancouver, University of British Columbia, 359 p.
Nadoll, P., Mauk, J., Leveille, R., and Koenig, A., 2015, Geochemistry of magnetite from porphyry Cu and skarn deposits in the southwestern United States: Mineralium Deposita, v. 50, p. 493–515.
Nakada, S., 1991, Magmatic processes in titanite-bearing dacites, central Andes of Chile and Bolivia: American Mineralogist, v. 91, p. 548–560.
Olade, M.A., 1977, Major element halos in granitic wall rocks of porphyry copper deposits, Guichon Creek batholith, British Columbia: Journal of Geochemical Exploration, v. 7, p. 59–71.
O'Reilly, S.Y., and Griffin, W.L., 2000, Apatite in the mantle: Implications for metasomatic processes and high heat production in Phanerozoic mantle: Lithos, v. 53, p. 217–232.
Pan, Y., Fleet, M.E., and Macrae, N.D., 1993, Oriented monazite inclusions in apatite porphyroblasts from the Hemlo gold deposit, Ontario, Canada: Mineralogical Magazine, v. 57, p. 697–707.
Parat, F., and Holtz, F., 2004, Sulfur partitioning between apatite and melt and the effect of sulfur on apatite solubility at oxidizing conditions: Contributions to Mineralogy and Petrology, v. 147, p. 201–212.
Pasero, M., Kampf, A. R., Ferraris, C., Pekov, I. V., Rakovan, J., and White, T. J., 2010, Nomenclature of the apatite supergroup minerals: European Journal of Mineralogy, v. 22, p. 163–179.
Pass, H.E., Cooke, D.R., Davidson, G., Maas R., Dipple, G., Rees, C., Ferreira, L., Taylor, C., and Deyell, C.L., 2014, Isotope geochemistry of the northeast zone, Mount Polley alkalic Cu-Au-Ag porphyry deposit, British Columbia: A case for carbonate assimilation: Economic Geology, v. 109, p. 859–890.
Patiño Douce, A.E., Roden, M.F., Chaumba, J., Fleisher, C., and Yogodzinski, G., 2011, Compositional variability of terrestrial mantle apatites, thermodynamic modeling of apatite volatile contents, and the halogen and water budgets of planetary mantles: Chemical Geology, v. 288, p. 14–31.
Peng, G., Luhr, J.F., and McGee, J.J., 1997, Factors controlling sulfur concentrations in volcanic apatite. American Mineralogist, v. 82, p. 1210–1224.
Piccoli, P.M., and Candela, P.A., 2002, Apatite in igneous systems: Reviews in Mineralogy and Geochemistry, v. 48, p. 255–292.
Piccoli, P., Candela, P., and Rivers, M., 2000, Interpreting magmatic processes from accessory phases: Titanite—a small-scale recorder of large-scale processes: Transactions of the Royal Society of Edingburgh, Earth Sciences, v. 9, p. 257–257.
Pouchou, J.L., and Pichoir, F., 1985, PAP $\phi(\rho Z)$ procedure for improved quantitative microanalysis, *in* Armstrong, J.T., ed., Microbeam analysis: San Francisco, CA, San Francisco Press, p.104–106.
Rabbia, O.M., Hernández, L.B., French, D.H., King, R.W., and Ayers, J.C., 2009, The El Teniente porphyry Cu-Mo deposit from a hydrothermal rutile perspective: Mineralium Deposita, v. 44, p. 849–866.
Rees, C., Gillstrom, G., Ferreira, L., Bjornson, L., and Taylor, C., 2014, Geology of the Mount Polley Intrusive Complex (final version): Geoscience BC, Report 2014–08.
Roegge, J.S., Logsdon, M.J., Young, H.S., Barr, H.B., Borcsik, M., and Holland, H.D., 1974, Halogens in apatite from the Providencia area, Mexico: Economic Geology, v. 69, p. 229–240.
Russell, J.K., Dipple, G.M., Lang, J.R., and Lueck, B., 1999, Major-element discrimination of titanium andradite from magmatic and hydrothermal environments: An example from the Canadian Cordillera: European Journal of Mineralogy, v. 11, p. 919–935.
Scott, K.M., 2005, Rutile geochemistry as a guide to porphyry Cu-Au mineralization, Northparkes, New South Wales, Australia; Geochemistry: Exploration, Environment, Analysis, v. 5, p. 247–253.
Selby, D., Nesbitt, B.E, Muehlenbachs, K., and Prochaska, W., 2000, Hydrothermal alteration and fluid chemistry of the Endako porphyry molybdenum deposit, British Columbia: Economic Geology, v. 95, p 183–202.

Sha, L.K., and Chappell, B.W., 1999. Apatite chemical composition determined by electron microprobe and laser-ablation inductively coupled plasma mass spectrometry, as a probe into granite petrogenesis: Geochimica et Cosmochimica Acta, v. 63, p. 3861–3881.

Sillitoe, R.H., 2010, Porphyry copper systems: Economic Geology, v. 105, p.3–41.

Stormer, J.C. Jr., Pierson, M.L., and Tacker, R.C., 1993, Variation of F and Cl X-ray intensity due to anisotropic diffusion in apatite during electron microprobe analysis: American Mineralogist, v. 78, 641–648.

Streck, M.J. and Dilles, J.H., 1998, Sulfur evolution of oxidized arc magmas as recorded in apatite from a porphyry copper batholith: Geology, v. 26, p. 523–526.

Sun, S.S., and McDonough, W.F., 1989, Chemical and isotopic systematics of oceanic basalts: implications for mantle composition and processes, *in* Saunders, A.D., and Norry, M.J., eds., Magmatism in the oceanic basins: Geological Society of London Special Publication 42, pp. 313–345.

Tepper, J.H., and Kuehner, S.M., 1999, Complex zoning in apatite from the Idaho batholith: A record of magma mixing and intracrystalline trace element diffusion: American Mineralogist, v. 84, p. 581–595.

Villeneuve, M., Whalen, J.B., Anderson, R.G., and Struik, L.C., 2001, The Endako batholith: episodic plutonism culminating in formation of the Endako porphyry molybdenite deposit, north-central British Columbia: Economic Geology, v. 96, p. 171–196.

Watson, J.L., 1969, Garnets of the Stikine copper's Galore Creek porphyry: B.Sc. thesis, Vancouver, University of British Columbia, 34 p.

Waychunas, G.A., 2002, Apatite luminescence: Reviews in Mineralogy and Geochemistry, v. 48, p. 710–742.

Webster, J.D., and Piccoli, P.M., 2015, Magmatic apatite: A powerful, yet deceptive, mineral: Elements, v. 11, p. 177–182.

Webster, J.D., Tappen, D., and Mandeville, C.W., 2009, Partitioning behavior of chlorine and fluorine in the system apatite-melt fluid: II. Felsic silicate systems at 200 MPa: Geochimica et Cosmochimica Acta, v. 73, p. 559–58.

Whalen, J.B., Anderson, R.G., Struik, L.C., and Villeneuve, M.E., 2001, Geochemistry and Nd isotopes of the François Lake plutonic suite, Endako batholith: Host and progenitor to the Endako molybdenum camp, central British Columbia; Canadian Journal of Earth Sciences, v. 38, p. 603–618.

Williams, S.A., and Cesbron, F.P., 1977, Rutile and apatite: Useful prospecting guides for porphyry copper deposits: Mineralogical Magazine, v. 41, p. 288–292.